International Journal of Thermophysics (2023) 44:55
https://doi.org/10.1007/s10765-023-03162-w

Assessment of Thermophysical Properties of Hybrid Nanoparticles [Graphene Nanoplatelets (GNPs) and Cellulose Nanocrystal (CNC)] in a Base Fluid for Heat Transfer Applications

M. Sandhya[1,2] · D. Ramasamy[1,2,3,4] · K. Kadirgama[1,2,3,4] · W. S. W. Harun[1] · R. Saidur[5,6]

Received: 20 August 2022 / Accepted: 24 January 2023 / Published online: 14 February 2023

Abstract

This article comprehensively investigates single (GNP) and hybrid nanofluids (GNPs/CNC nanoparticles), including nanofluid preparation and thermophysical properties. Nanoparticles were characterized using field emission scanning electron microscope, transmission electron microscope and X-ray diffraction analysis. A two-step approach is used in nanofluid preparation, and various analytical practices determine the prepared nanofluids. The range of the temperature set to measure the thermal conductivity of nanofluids is 20 °C to 50 °C using the ASTM D2717–95 norm. The present study range of the nanofluid volume concentration is from 0.01 vol% to 0.2 vol%. For the single GNP nanofluid, temperatures at room level indicated the thermal conductivity value in the range of 0.366 $W{\cdot}m^{-1}{\cdot}K^{-1}$ to 0.441 $W{\cdot}m^{-1}{\cdot}K^{-1}$; for hybrid nanofluid, the thermal conductivity values are 0.501 $W{\cdot}m^{-1}{\cdot}K^{-1}$ to 0.551 $W{\cdot}m^{-1}{\cdot}K^{-1}$. In addition, nanofluid's viscosity, density and specific heat capacity are the experimental density value increased with the concentration of nanoparticles with 1050 kg/m^3 and 1060 kg/m^3 for 0.01 % concentration of single/hybrid nanofluids, respectively. Finally, based on the findings, it can be determined that the thermal properties of the selected nanoparticles are beneficial, and hybrid nanofluid is an acceptable alternative to conventional/water-based fluids in terms of thermal properties in operational systems.

Keywords Crystal nanocellulose · Graphene nanoplatelets · Hybrids · Thermal conductivity · Viscosity

✉ M. Sandhya
madderla.sandhya@gmail.com

Extended author information available on the last page of the article

1 Introduction

The utilization of solid nanoscale particles distributed in the base fluid is an advanced approach for increasing the thermal functioning of heat transfer solutions. Nanofluids in this research were considered as a modern heat transfer solution by combining solid nanometre-sized particles of graphene nanoplatelets/cellulose nanocrystals (GNPs/CNC) at minimal concentrations with the base fluid (ethylene glycol:water; 60:40). Heat transfer is a concern of practical significance and prominence in the industries [1]. The potential of fluids to heat flow is a significant responsibility in the quantity of heat loss and thermal conduction in general. Many industries rely on water, ethylene glycol and oil [2, 3] fluids. Considering current innovations and new technologies in specific sectors, it is crucial the increase thermal properties ability with this type of fluids. Researchers are currently experimenting with nanofluids and ensuring the appropriate stabilization of nanoparticles in base fluids to enhance their heat properties [4].

Nanoparticles are distributed in a "traditional" operating fluid such as water or the antifreeze (ethylene glycol) to create an efficient substitute working fluid for enhanced heat transfer called "nanofluid" [5]. Choi and Eastman [6] first proposed the term "nanofluid" in 1995, referring to nanoparticles with diameters of 1–100 nm in base fluids. Investigators have discovered that application to a working fluid by introducing nanoparticles changes its thermophysical properties dramatically in the new decade [7]. The changed thermal properties of the dispersed nanoparticles in the base fluid in evaluation to the traditional fluid have resulted in some noteworthy improvements in the nanofluids' thermal properties [8], like thermal conductivity and convective efficiency of the heat transfer (CHT). Nanoparticles of metal or metal oxides, such as aluminium oxide (Al_2O_3), copper (Cu), copper oxide (CuO), zinc oxide (ZnO), silver (Ag), cerium oxide (CeO_2), aluminium (Al), nickel, iron (Fe) and titanium oxide (TiO_2), or carbon-based particles, such as carbon nanotubes (CNTs), fullerenes, graphene, graphite quantum dots, nanodiamonds, graphene oxide (GO) and graphene nanoplatelets (GNPs), are few of the examples of nanoparticles [9]. Since single-/multi-wall carbon nanotubes, graphite and graphene/graphene oxide are carbon-based nanoparticles and are sometimes referred to as effective nanoparticles, many scientists are currently focusing on them to develop nanofluids with high-aspect-ratio nanoparticles with improved thermal, mechanical and catalytic characteristics [10]. All nanoparticles with carbon base have superior thermal conductivity, and these nanofluids have significantly improved thermal properties like thermal conductivity, including coefficients of heat transfer. For improving the heat transfer coefficient and thermal conductivity of heat-exchanging fluid, most of the preliminary research has been conducted on single/mononanoparticles because of its unusual physical or thermal properties and mechanical or electrical properties [11, 12]. Graphene has fascinated a lot of consideration as a two-dimensional carbon atom with a single layer [13]. Graphene nanoplatelets, on the other hand (which are made up of numerous layers of graphene), bring the advantages together of monolayer properties, like the area of surface a high and excellent thermal conductivity,

alongside tightly packed graphitic carbon advantages, also such as strong, stable nature and low budget. Due to strong van der Waals interactions, GNPs are likely to accumulate between the cause of large specific surface area [14, 15]. Figure 1 shows the essential properties related to nanofluids for the thermal application obtained from the Scopus data.

"Nanocomposite" refers to synthesizing at least two distinct nanoparticles into one. The author Sundar Singh [16] produced MWCNT-Fe_3O_4 nanocomposite, developed a hybrid nanofluid and achieved a 29 % increase in thermal conductivity at 0.3 % concentration (volume) in water at 60 °C. Additionally, thermal-based performance of the hybrid nanofluids is higher than single nanofluids. The authors Theres Baby and Sundara [17] developed a hybrid nanofluid and observed an increase of 8 % in thermal conductivity for Ag/MWCNT-HEG at a volume fraction of 0.04 % and 25 °C. Amiri and Shanbedi [18] studied the properties of the prepared nanofluids of MWCNT–Ag nanocomposites for thermal conductivity and concluded that the hybrid nanoparticles attained the highest thermal conductivity for the heat exchanger application in a cooling system. The covalent and noncovalent polymerization methods are utilized and discovered that the covalent method is better for sustained thermophysical properties of nanofluid. As graphene nanoplatelets are hydrophobic in nature [19], the functionalization process which used to generate suspension of stable nanofluids with graphene is appropriate for nanofluid applications. With a yearly output of approximately 7.6×10^{10} tons, cellulose is the

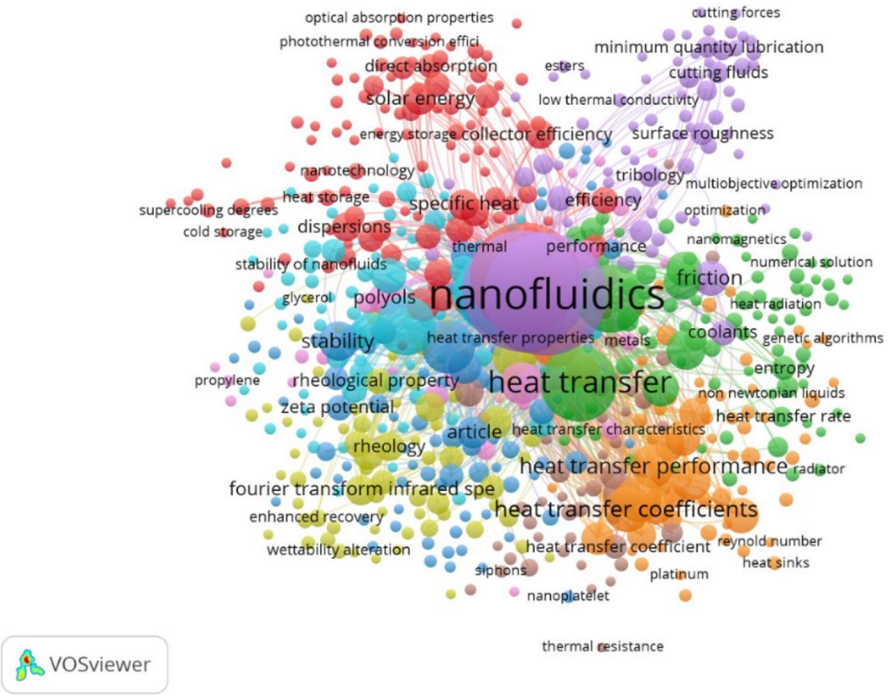

Fig. 1 Bibliographic representation of accomplished properties related to nanofluids

most abundant renewable organic substance [20]. Nanosized cellulose has recently attracted attention due to its extraordinarily high specific strength and modulus, low density, chemical adaptability, renewable "green" nature and affordable cost [21]. Few research has been done on finding the mechanical properties of the prepared hybrid nanocellulose fluid, but there is no or limited research on hybrid cellulose for thermophysical properties for thermal application [22, 23]. Cellulose nanocrystals (CNC) are in fibrillar forms, with a diameter of about 5 nm and a length that varies depending on their source and fabrication process [24]. Cellulose, the most common organic substance from the ecosystem, is renewable, biodegradable, biocompatible, nontoxic and environmentally friendly. This is attributable to its recyclability and cytocompatibility [25], has drawn increasing attention in several disciplines and could serve as a notable alternative to thermal applications. The benefits of cellulose can also be advanced by investigating its nonmetric size, which results in nanocellulose, which is regarded as a capable class of forthcoming materials expected of its remarkable physicochemical capabilities. Nanocellulose has a low density, dilatation morphology, inertness, wide surface area and aspect ratio and is abundant and easy to bio-conjugate. Due to their unique physicochemical, mechanical, thermal, rheological and optical properties, CNC-based nanomaterials have been widely studied [26–28]. CNC could provide acceptable features to hybridization or nanocomposites (metallic, ceramics and polymeric), however, at low concentrations for a wide range of applications. Fullerenes, carbon nanotube (single-walled, double-walled, few-walled or multi-walled), nanodiamonds, as well as graphene-based materials like graphene, oxide form of graphene, reduced form of graphene oxide and graphene quantum dots have evolved into a original category of hybrid materials with a synergetic effect or synergetic effect in a variety of applications [25, 29]. Despite the fact that several potentially possible techniques to produce effective graphene nanoplatelets are now being developed, there are still several practical difficulties to overcome. GNPs, for example, are further normally generated from aqueous dispersals, although they can effortlessly agglomerate. This type of agglomeration can limit surface area which has detrimental impact on properties. With this resultant by the addition of CNC not only overcomes this disadvantage due to its exceptional disseminative properties, but similarly converses additional assistances to the resulting GNPs/CNC hybrids, such as quick dispersion and thermal stability, as well as improved adsorption capability, photothermal interaction, sustainability, intrinsic luminosity and diffraction, optical transparency and thermal conductivity [30–32]. Considering these facts, using CNC as a companion material in GNP nanoparticles could be more effective and beneficial in improving the nanocomposite's thermal conductivity and its properties. The fluid mixture of 60 % ethylene glycol and 40 % water is most frequently employed by many researchers for improved heat transfer [33–37]. To investigate the thermophysical characteristics of such nanofluids, a brief literature survey is carried out and presented in the previous article [9]. We detail the preparation and thermal properties of GNPs/CNC hybrid fluids in this study. This paper presents a forward perspective on GNPs/CNC hybrids for various applications. Nonetheless, the progression of GNPs/CNC hybrid-based nanomaterials is a comparatively innovative belief that is largely restricted to scholarly disciplines. However, it is expected that several hybrid nanofluid (graphene-based) research will

become more attractive in the potential, attracting more study consideration not only in several functions but additionally in achieving multifunctional systems and opening new perceptions. Furthermore, the sensible implementation of such hybrids as next group materials necessitates significant functional and performance enhancements. The current study emphasizes on comparison of nanofluid thermophysical properties with single and hybrid graphene-based nanofluid. As there are no data available in the literature for the novel work as this kind on the thermophysical properties assessment of hybrid nanoparticles consists of the graphene nanoplatelets and cellulose nanocrystals in a base fluid of ethylene glycol and water at a ratio of 60:40.

2 Methodology

This research process offers comprehensive details about the analysis, the materials and equipment utilized for the characterization of nanofluids (water and ethylene glycol-based GNP and GNPs/CNC), nanoparticles of single/hybrid and accompanied by an examination of stability.

2.1 Materials

In this investigation, graphene nanoplatelets (GNPs) with 800 $m^2 \cdot g^{-1}$ specific surface area (S.A) were employed, which were purchased from Nanografi Nanotechnology (USA) with 99.9 % purity, 3 nm size and 1.5 m in diameter, and crystalline nanocellulose from the country Malaysia by MY Biomass Sdn. Bhd. The nanoparticles are weighed employing the Internal Sartorius Analytical Balance (Model: BSA24S-CW). A magnetic stirrer with a rotating magnetic probe (Thermo Fisher, USA) and an ultrasonicator (CE ISO Ultrasonic Homogenizer Sonicator Processor Cell Disruptor Mixer 20-1000 mL with power 950W and 20 kHz power supply) is used to distribute the nanoparticles uniformly. The hydrophilic nature of CNC pulp form is quite a challenging and necessary chore to separate in the form of powder. Spray-drying approach using a tiny fan is employed for CNC handling in the form of powder. When the pulp or suspensions reached into connection with heated air from the nozzle spray dryer's entering space, the moisture quickly evaporated, resulting in a steady CNCs flake. The flakes of CNC are collected and ground into powder. The specific parameters of the obtained CNC nanoparticles are: crystallinity index with 80 %, 100–150 nm crystal length, 9–14 nm crystal diameter and the hydrodynamic diameter 150 nm. Table 1 displays the physical properties of certain graphene nanoplatelets and CNC nanoparticles, and Table 2 gives information about the thermophysical properties of base fluid water and ethylene glycol at 20 °C temperature.

2.2 Preparation of Nanofluid

At 0.01 %, 0.05 %, 0.1 % and 0.2 % volume concentration, the graphene nanoplatelets are scattered in the base fluid (60:40) using a magnetic stirrer for about 2 h and later the probe (φ13mm diameter) of the ultrasonication. Using Eq. 1, the density of hybrid

Table 1 Physical form of properties of nanoparticles

Properties	GNP	CNC
Colour	Black	White (dry powder)
Purity	99.9 %	–
Density ($kg{\cdot}m^{-3}$)	2267	1050
Structure	Platelet-shaped sheets	Crystalline form
Specific surface area ($m^2{\cdot}g^{-1}$)	800	–

Nanografi Nanotechnology (USA), MY Biomass Sdn. Bhd (MALAYSIA)

Table 2 Base fluid thermophysical properties at 20 °C [38, 39]

Properties	Water (H_2O)	Ethylene glycol ($C_2H_6O_2$)	Ethylene glycol/water (60:40)
Vapour pressure (kPa)	3.169	0.007	–
Molar mass ($g{\cdot}mol^{-1}$)	18.0153	62.07	–
Density ($kg{\cdot}m^{-3}$)	1000	1100	1086.23
Thermal conductivity ($W{\cdot}m^{-1}{\cdot}K^{-1}$)	0.608	0.258	0.335
Specific heat ($J{\cdot}kg^{-1}{\cdot}K^{-1}$)	4178	2348	3079.2
Viscosity (mPa·s)	1.0015	16.59	5.9134

nanoparticles is calculated [40]. Carbon-based hydrophobic nanoparticles cannot be sustainably distributed in the base fluid. Graphene nanoplatelets, as a result of their electrical and thermal conductions, are in graphite form. The GNPs can be scattered in a medium with a stirrer and sonication through a probe without utilizing surfactants. Therefore, 5 h of ultrasonication time was used to make the particles properly disperse and stable with a power utilization of 50 %. Likewise, a hybrid nanofluid prepares the particles GNPs/CNCs at a 1:1 ratio and is distributed in the base fluid through a magnetic stirrer. This high-speed stirrer operated at a range of 400–500 rpm until proper blending/mixing for about 120–180 min and altered every 15 min, followed by an ultrasonication procedure with a probe for 5 h with a power output of 50 % with interval gap of 5 min after every 15 min of sonication process to uphold the temperature of the fluid. This discontinuity prevents nanofluids from heating up and losing the properties of particles. For hybrid nanoparticles, the weight of nanoparticles was validated using Eq. 2 [30, 41].

$$\rho_{GNP/CNC} = \frac{\phi_{GNP}\rho_{GNP} + \phi_{CNC}\rho_{CNC}}{\phi_{total}} \tag{1}$$

$$WGNP/CNC = \left(\frac{\varphi}{100-\varphi}\right) \times \left(\frac{\rho(GNP/CNC)}{\rho(bf)}\right) Wbf \tag{2}$$

where "W" is weight, "φ" implies the concentration of single/hybrid nanofluids, "ρ" defines the density and "bf" represents the base fluid, respectively. Figure 2 provides a schematic illustration of the development of nanofluid by using the two-step preparation method. Several researchers use two-step preparation method. The detailed preparation method for the hybrid nanofluid is discussed in the previously published article on the preparation of hybrid nanofluid [42, 43].

2.3 Measurement Methods

2.3.1 Evaluation of the Stability

The clustered nanoparticles get agglomerated and interrupt the hybrid nanofluids' stability due to their large surface area, which is a critical condition for their utilization. The GNPs/CNC nanoparticle's stability and dispersibility in the nanofluids were studied in previous work [42] by applying the sedimentation method with photographs captured at different periods, using UV–Vis spectroscopy and zeta potential analysis. For proper light transmission, all the samples with base fluid are diluted. The single/hybrid nanofluid zeta potential is determined using the Anton Paar light sizer 500. In nanofluid dispersion, the zeta potential measurement displays the repulsion degree amongst nearby particles with a similar control.

2.3.2 Characterization

The characterization of nanoparticle microstructure in the nanofluids is done using a transmission electron microscope (TEM). The particle size and dispersion of W/EG developed GNP and hybrid nanofluids of GNP were measured using a digital TEM. Before TEM examination, the samples of the hybrid nanofluids are sonicated for 15 min. TEM apparatus (Tecnai G2 20 S-TWIN, USA) employing 210 kV of accelerated voltage evaluated the solution of nanofluid constituted with GNPs/CNC of the base fluid. GNP and GNPs/CNC nanofluids remained analysed by means of

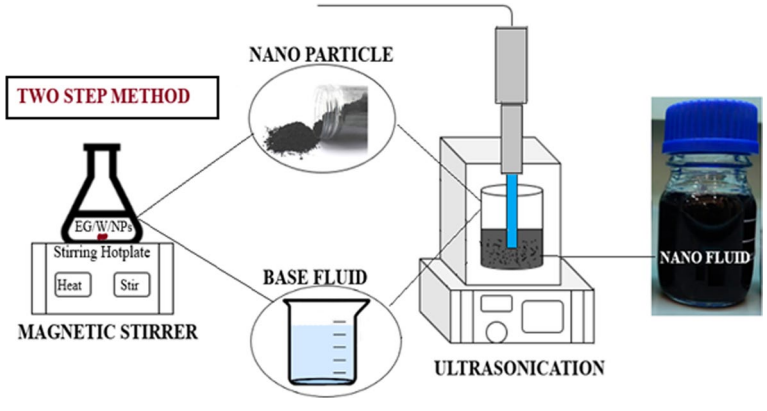

Fig. 2 Two-step preparation method representation [42]

an X-ray diffractometer (Rigaku D/MAX-2500PC, Japan) with Cu K α radiation (λ = 1.54056 Å) at 40 kV and 30 mA, with 0.02° rate of the scan. The nanoparticle's phase was assessed using X-ray diffraction (XRD) analysis. The produced nanofluid trials are coated to assess apparent morphology for microstructure characterization. SEM scanning electron microscopy (HITACHI/TM 3030 PLUS, Czech Republic) was used to examine the diffusion of nanoparticles in the fluid. Field emission scanning electron microscopy (FESEM, Zeiss Sigma HD VP, Germany) was used to investigate the structure of developed filaments at 0.5 kV acceleration voltage. Prior to observation, each sample had platinum-sputtered. The samples were morphologically inspected before being seen using a FESEM scope for capturing the topographical representations of the powder as received [44, 45].

2.3.3 Thermal Conductivity Measurement

Various strategies for evaluating the thermal conductivity of nanofluids have been recommended. Transients hot wire is highly accurate and quick of all these approaches (THW). In this research, for measuring thermal conductivity, a hot wire-type KD2-Pro (Decagon Devices Inc., USA) is used for GNP/base fluid (W/EG), and GNPs/CNC-based hybrid nanofluid is established. Table 3 lists studies that indicate the thermal conductivity estimates obtained by authors at distinct volume concentrations. These thermal conductivity values are used to validate the thermal conductivity estimates attained in the present study at different temperatures and volume concentrations.

Temperature bath (WNB7-MEMMERT, Germany) was used for sustaining and monitoring the thermal conductivity measurement by temperature control. Probe vibration must be regulated to minimize experimental errors. To position vertically the KS-1 probe in the middle point of the sample vial, a horizontal support was mounted adjacent to the temperature bath. To examine the reproducibility of the data, the repetitive measurements were taken twenty times in all planned volume concentrations and temperatures in a 5-min intervening period. Table 4 presents a few specifications of thermal conductivity measuring device KD2 Pro information.

2.4 Viscosity

All nanofluid's viscosity was measured using a rheometer (Brookfield DV-I prime viscometer) in the temperature range of 20 to 50 °C with different volume concentrations. An RST coaxial cylinder rheometer is attached to a circulating water jacket for different purposes, including determining the temperature range. The rheometer can detect temperatures between − 200 °C and + 180 °C and viscosities between 0.0001 Pa·s and 5.4×10^6 Pa·s. The experiment was conducted in a steady-state situation. Rotational measurement with a controlled shear rate was used as the method of measurement. The base fluids' viscosity was quantified to authenticate the rheometer, and the results were assessed to ASHRAE standard data. The viscosity is measured with 15.7 mL of fluid, and the results are compiled in a computer connected to an RST rheometer. To reduce the experimental error, five precision readings were

Table 3 Nanofluid thermal conductivity enhancement summary

NPs	Concentration (%)	Thermal conductivity ($W \cdot m^{-1} \cdot K^{-1}$)				References
		30 °C	40 °C	50 °C	60 °C	
Graphene nanoplatelets	0.01	0.31	0.34	0.36	0.37	[47]
	0.05	0.38	0.4	0.41	0.42	
	0.1	0.43	0.44	0.45	0.46	
	0.2	0.46	0.48	0.5	0.52	
Graphene	0.05	1.02	1.019	1.03	N/A	[48]
	0.08	1.052	1.066	1.078		
Graphene	0.124	0.315	0.318	0.319	0.325	[49]
	0.207	0.324	0.327	0.33	0.339	
	0.395	0.335	0.339	0.342	0.345	
	0.1	0.72	0.77			
Graphene nanoparticles ($750\ m^2 \cdot g^{-1}$)	0.024	0.68	0.71	N/A		[50]
	0.05	0.71	0.75			
	0.1	0.75	0.8			
Graphene NP-Ag	0.2	0.63	0.651	N/A		[51]
	1.0	0.72	0.77			
Graphene nanoplatelets	0.1	0.5	0.51	0.525	N/A	[34]
	0.2	0.54	0.55	0.565		
	0.3	0.62	0.64	0.66		
Graphene nanoplatelets	0.1	0.187	0.18	0.179	0.17	[52]
	0.25	0.20	0.20	0.199	0.19	
	0.5	0.215	0.213	0.21	0.209	

Table 4 Specifications of the thermal conductivity measurement device (KD2 Pro)

Accuracy ± 5 %	Thermal conductivity
Range of operation	0–50 °C
Measurement range	0.02–2 $W \cdot m^{-1} \cdot K^{-1}$
KS-1 sensor	Needle length: 60 mm
	Needle diameter: 1.3 mm

acquired and averaged. Previously, several researchers used the Brookfield rheometer to determine the viscosity [53–55].

2.5 Density and Specific Heat Measurement

The pumping power, friction factor, Reynolds number and other properties of nanofluids were all affected due to their density. This work uses a digital density meter to test the density of GNP and GNPs/CNC nanofluids with varying volume concentrations, similar to prior investigations by various researchers. The density meter used here is a KEM (model DA-640) from Kem Kyoto Electronics Co. Ltd. The

density). The measuring range on this meter is 0.0000 gm·cm^{-3} to 3.000 gm·cm^{-3}, with a ± 0.0001 gm·cm^{-3} precision and repeatability of 0.00005 density (gm/cm^3). The temperature range for utilizing the meter is 35 °C, with a humidity level of 85 % RH or less. The density is measured using an ASTM D4052-18 digital density meter, which is recognized as a standard test method for density, relative density and API gravity of liquids [56–58]. Differential scanning calorimetry (DSC) is a sensitive method used in determining the specific heat capacity of viscoelastic fluids. PerkinElmer, Inc.'s DSC (model DSC 8000) was utilized to measure particular heat in this study. The specific heat capacity of the base fluid and GNPs/CNC nanofluids was examined at room temperature. The measurement solution was placed in an aluminium pan and weighed on an electrical balance with a precision: of 0.0001 before being contained with an aluminium cover and closed with a universal crimper press. An empty pan filled with sapphire reference was placed in DSC before the actual sample measurement to get baseline and reference data. Following that, the sample pan was put in DSC beside an empty pan as a control. Following the standard DSC test procedure ASTM-E1269. The temperature range was set with a 10 °C/min temperature difference. For each sample, a minimum of 6 min was required. This test was carried out for all nanofluid and base fluid volume concentrations. The generated values are saved on a computer that is linked to DSC. Previous studies employed DSC to conduct precise heat measurement tests on nanofluids [59–62].

3 Results and Discussions

3.1 Nanofluid Preparation, Characterization and Stability

The preparation method is a two-step method for single graphene nanoplatelets and hybrid nanoparticle dispersal. In the Faculty of Mechanical Engineering's Advanced Automotive Liquid Lab (AALL) at the Universiti of Malaysia Pahang, the needed graphene nanoplatelets and nanocellulose hybrid nanofluid were prepared successfully. Over a 5 h ultrasonication duration followed by magnetic stirring, ultrasonication is the most influential way to generate a very balanced dispersion of GNPs and hybrid nanoparticles. Figure 3 displays diffraction peaks for the CNC and graphene refraction planes, respectively, at $2\theta = 15.7°$, 22.8°, 34.6° and 26.3°, 43.9°, 54.1°. The peak in graphene at $2\theta = 26.35°$ reflected a typical graphitic carbon diffraction pattern [51, 63, 64].

Furthermore, the connected carbon in cellulosic form was demonstrated by a negatively diffracted signal at $2\theta = 22.83°$. It further shows that the CNC peak intensity is higher than that of graphene's peak. The field emission scanning electron microscopy images for GNPs/CNC hybrid nanofluids are shown in Fig. 4a and b. A consistent dendrite forms uneven structure noticed for GNPs with platelet structure and CNC with porous microstructure with homogeneity and uniformity. TEM examination of GNPs/CNC hybrid nanofluid morphology and dispersion is depicted in Fig. 4c and d. It shows distributed GNPs together with a CNC base due to the transparency. As the concentration of nanoparticles increases, it reduces clarity, as shown in the image, suggesting agglomeration. The cellulose nanocrystals' structure

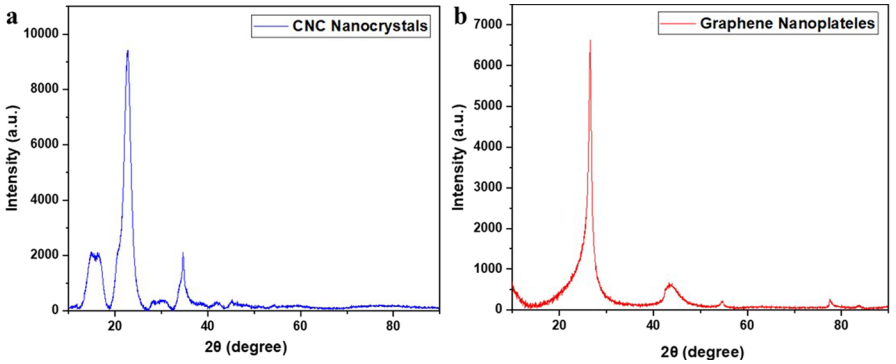

Fig. 3 Analysis of XRD (a) CNC and (b) nanoparticles of graphene nanoplatelets

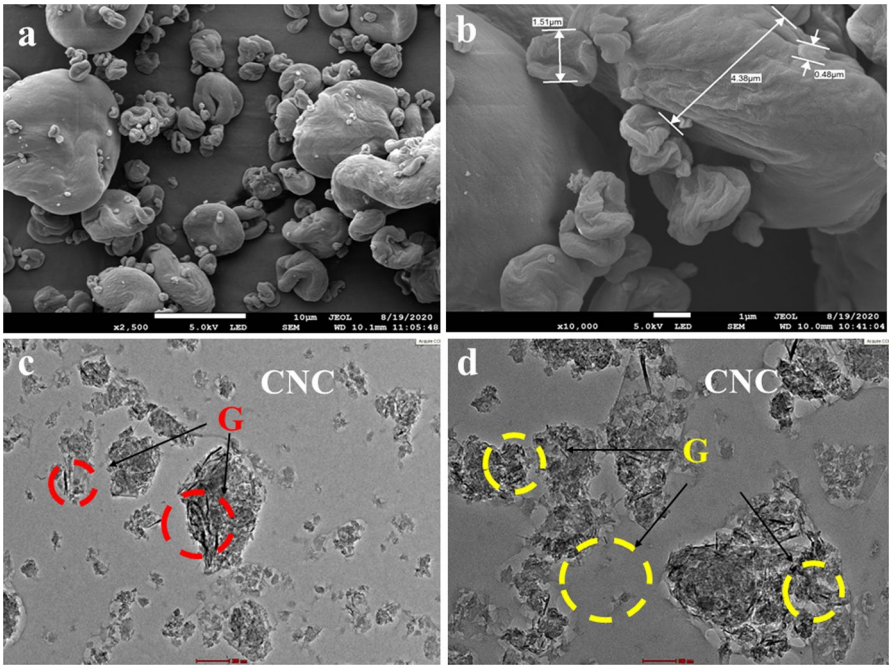

Fig. 4 Images of FESEM of (a) GNPs/CNC hybrid nanofluid at ×2500 (b) at ×10 000 magnification. (c) TEM images of hybrid nanofluids 0.2 % GNPs/CNC at lower enlargement, (d) at higher magnifications

and graphene nanoplatelets' dispersion in the base fluid (EG/W) are investigated using microstructure TEM analysis. Graphene nanoplatelets with platelet structure and CNC with a clear and gentle exterior in the base fluid display fragile structure behaviour. Finally, the dispersed GNPs/CNC morphology reveals that the nanoparticles were well prepared and distributed in the ethylene glycol and water base fluid. The information related to the preparation of the nanofluid in detail can be found in

the previous article by authors related to the preparation, characterization and longevity (stability) of the single and hybrid nanofluids [42].

3.2 Thermal conductivity

KD2 Pro thermal properties analyser was utilized for assessing thermal conductivity between 20 °C and 50 °C. Validation is a process of calculating the parameters in any laboratory work; the instrument must be adjusted. To calibrate the unit, the manufacturer of the KD2 Pro recommends using a standard sample of glycerine. The device's accuracy must be tested before calculating the nanofluid's final thermal conductivity tests. Besides, the estimated data of base fluid was compared with the data presented by different authors [46, 65]. The effect of temperature and the concentration based on volume for the thermal conductivity of graphene nanoplatelets and hybrid GNPs/CNC nanofluids has been extensively investigated. The different volume percentages have variable thermal conductivity. GNPs/CNC hybrid nanofluid samples are tested at temperatures ranging from 20 °C to 50 °C, as shown in Fig. 5. The thermal conductivity of graphene nanofluids is shown in Fig. 5 as a function of concentration in the 0.01–0.2 volume percentage range at various temperatures with the ASHRAE base data for the comparative analysis. The result of the thermal conductivity of base fluid is in good qualitative agreement with ASHRAE data with a maximum difference of 4 %.

Low-weight percentages are chosen to avoid an increase in effective viscosity and sedimentation. The thermal conductivity increases as the concentration of graphene increases, which is to be expected. At a concentration of 0.01 %, the

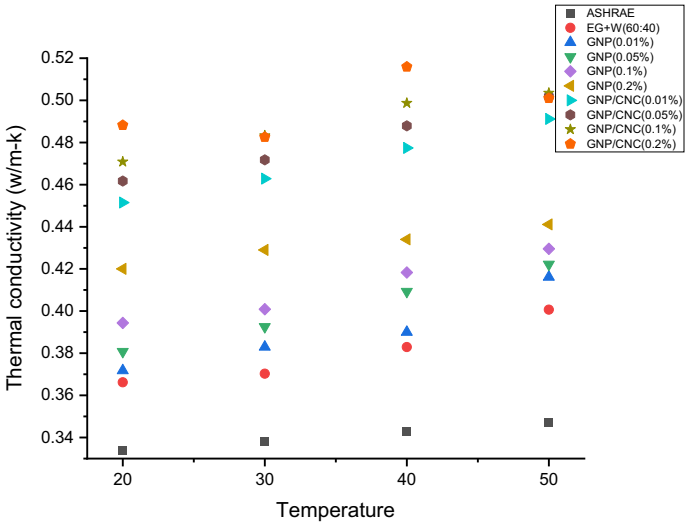

Fig. 5 Thermal conductivity of GNP and GNPs/CNC nanofluids at different concentrations and temperature

thermal conductivity value is 0.3716 $W{\cdot}m^{-1}{\cdot}K^{-1}$ for graphene nanoplatelet nanofluid at 20 °C. At a concentration of 0.2 %, the maximum enhancement was 27 % with 0.4411 $W{\cdot}m^{-1}{\cdot}K^{-1}$ at 50 °C. At the same temperature from the above image, it contrasts the enhancement of thermal conductivity with concentrations of graphene nanoplatelets and hybrid graphene nanoplatelet nanofluids. It is clear that the rate of enhancement increases with the concentration of graphene and cellulose nanocrystals, compared to metallic and ceramic nanofluids and is much superior to them. Temperature and volume concentration significantly increase the thermal conductivity of graphene nanoplatelet nanofluids.

This is because graphene nanofluids contain particles of varying sizes. According to percolation theory, the larger particles contribute to forming a network-like chain structure. Brownian motion is contributed by the smaller particles, which travel spontaneously. As the temperature rises, Brownian motion creates microconvection, which increases thermal conductivity. This has led to the strong suggestion of a hybrid character for thermal conduction in graphene nanofluids comprising microconvection and diffusion phenomena. With increases in weight proportion and temperature, the rise in thermal conductivity is nonlinear. The nonlinearity/linearity of the variability of thermal conductivity concerning weight fractions is influenced by the characteristics of the hybrid nanoparticles and even the base fluid. The increase in thermal conductivity is 14.91 % at 20 °C and about 17.77 % at 40 °C when using a 0.01 % weight concentration of GNPs/CNC nanofluid. The high thermal conductivity of GNPs/CNC nanoparticles results in an increase in effective thermal conductivity. The spacing amongst nanoparticles (unrestricted passage) reduces as the volume fraction of nanoparticles increases. It occurs as a result of the percolation effect.

Other studies have also seen an increase in the thermal conductivity of carbon-based nanofluids as the weight concentration increases [66, 67]. The reason for the increase in thermal conductivity of nanofluids so vividly is that nanoparticles move in a Brownian approach, molecular level of the liquid at /particle contact layers, the nature of heat transmission of the nanoparticles, and the impact of nanoparticle clustering are some of the hypothesized mechanisms [68]. They concluded that Brownian motion could be ignored because thermal diffusion has a more significant influence than Brownian diffusion though it is the measure of immobile nanofluids. Although many contributing factors have been examined, such as the liquid–solid interfacial region, Brownian motion, charge carrier status and ballistic dielectric transport, no overarching mechanism to govern the exceptional behaviour patterns of nanofluids, counting that of significantly improved effective thermal conductivity, has been discovered. Like graphene nanofluid thermal conductivity, there is an increase in the hybrid GNPs/CNC hybrid nanofluids with an increase in volume concentration from 0.01 % to 0.2 %. The thermal conductivity value is recorded at 40 °C for 0.2 % at 0.465 $W{\cdot}m^{-1}{\cdot}K^{-1}$. At the same volumetric concentration and temperature compared to single and hybrid nanofluid, there is an increase of 5.2 % and 13.3 % concerning base fluid. Table 5 gives the validation of the present study by comparing it with the previous studies based on graphene nanoparticles and hybrid nanoparticles. The present study base fluid experimental values at 60:40 EG: W ratio agree well with the author Sundar, Singh [69] at the same base fluid ratio

Table 5 Thermal conductivity of single and hybrid nanofluids attained by various researchers

Nanoparticle	Concentration/temperature	k_{NF}/k_{BF}	References
Graphene nanoplatelets/EG-W	φ = 0.01 % vol/50 °C	1.038	Present study
	φ = 0.05 % vol/50 °C	1.053	Present study
	φ = 0.1 % vol/50 °C	1.071	Present study
	φ = 0.2 % vol/50 °C	1.100	Present study
Graphene nanoplatelets-CNC/EG-W	φ = 0.01 % vol/50 °C	1.225	Present study
	φ = 0.05 % vol/50 °C	1.252	Present study
	φ = 0.1 % vol/50 °C	1.256	Present study
	φ = 0.2 % vol/50 °C	1.250	Present study
3D graphene/EG	φ = 0.1 % wt/25 °C	1.149	Bing, Yang [70]
Graphene/DIW	φ = 0.1 % wt/25 °C	1.416	Ghozatloo, Rashidi [71]
Graphene nanoplatelets/EG	φ = 0.5 % vol/35 °C	1.208	Selvam, Lal [72]
		1.160	
	φ = 0.1 % wt/60 °C (500 $m^2 \cdot g^{-1}$ GNP)	1.287	Iranmanesh, Mehrali [73]
	φ = 0.1 % wt/60 °C (750 $m^2 \cdot g^{-1}$ GNP)	1.307	
Graphene/EG/DIW	φ = 0.2 % wt/25 °C	1.092	Contreras, Oliveira [74]
Graphene nanoplatelets	φ = 1 % wt/25 °C (750 $m^2 \cdot g^{-1}$)	1.211	Wang, Wu [75]
Hybrid graphene wrapped MWNT			
TiO_2/graphene/W	φ = 0.25 % vol/25 °C	1.098	Bakhtiari, Kamkari [76]
	φ = 0.25 % vol/55 °C	1.138	
Al_2O_3/graphene oxide/W	φ = 0.25 % vol/50 °C	1.125	Taherialekouhi, Rasouli [77]
Fe-Si/DW	φ = 0.25wt %/50 °C	1.109	Huminic, Huminic [78]
Graphene oxide/Co_3O_4/W	φ = 0.2wt %/50 °C	1.156	Sundar, Singh [69]
Graphene oxide/Co_3O_4/EG	φ = 0.2vol %/50 °C	1.113	Sundar, Singh [69]
Graphene oxide/Co_3O_4/EG/W	φ = 0.2vol %/50 °C	1.120	Sundar, Singh [69]
Graphene oxide-CuO/EG-W	φ = 0.2vol %/50 °C	1.094	Rostami, Nadooshan [79]
Graphene nanoplatelets-platinum/DW	φ = 0.1vol %/40 °C	1.174	Yarmand, Gharehkhani [44]

at temperatures varying from 20 °C to 50 °C. The thermal conductivity values are compared at around equal concentrations and temperatures to give a clearer vision of the present study.

3.3 Viscosity

The viscosity of EG/distilled water (base fluid) at a ratio of 60:40, GNP and GNPs/CNC hybrid nanofluids at varying volume concentrations and temperatures ranging from 20 °C to 50 °C is shown in Fig. 6. Viscosity has adverse effects on two factors for pressure drop and pumping power constraints, similar to density. Because of

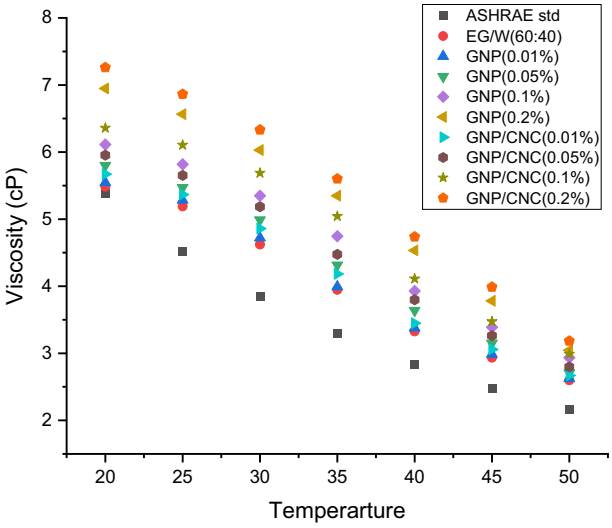

Fig. 6 Viscosity of prepared nanofluids at different concentrations and temperatures

NPs/surface collisions and other interlayer resistance and interfacial forces, the presence of nanoparticles in the base fluid, i.e. constituting to the nanofluid, increases friction at the fluid/surface contact. At 20 °C, the measured viscosity of the base fluid (EG/water) is 5.485 (mPa·s), which is consistent with literature values. Since the increasing concentration directly affects the fluid internal shear rate, the viscosity of nanofluids rises as the volume fraction of nanofluids rises [80]. The viscosity reduces as the temperature rises, as intermolecular and interparticle adhesion forces weaken. When 0.2 % volume concentration of GNP nanofluid is compared to the viscosity of EG/water at 20 °C, the viscosity increases by around 21 %.

Similarly, there is an increase in viscosity by 24.5 % at 0.2 % volume concentration of hybrid nanofluid (GNPs/CNC) at 20 °C. The viscosity values diminish as the temperature rises. The increased viscosity value at 0.2 % volume concentration of GNP nanofluid at 50 °C is only 14.7 % compared with base fluid and that of hybrid nanofluid of GNPs/CNC at 0.2 % volume concentration at 50 °C is 18.3 %. The GNPs/CNC sample had the highest stability and caused the greatest increase in the average viscosity of the base fluid. High colloidal stability and the lowest rise in base fluid viscosity are two of the most important factors to consider when using nanofluids as operating fluids in heat transfer applications. Accordingly, by the viscosity values, the highest concentration of nanoparticles (single/hybrid) can be considered effective.

Because a considerable amount of nanomaterial has been disseminated, the friction factor appears high at high volume concentrations. The friction factor improves the value of dynamic viscosity. However, as the nanofluid temperature rises, the intermolecular adhesion force weakens, resulting in a lower dynamic viscosity value [80]. Figure 7 depicts the viscosity ratio of 60:40 (EG: W)-based fluids, as well as from author Sundar, Singh [69] data for 60:40 (EG: W)-based fluids for the

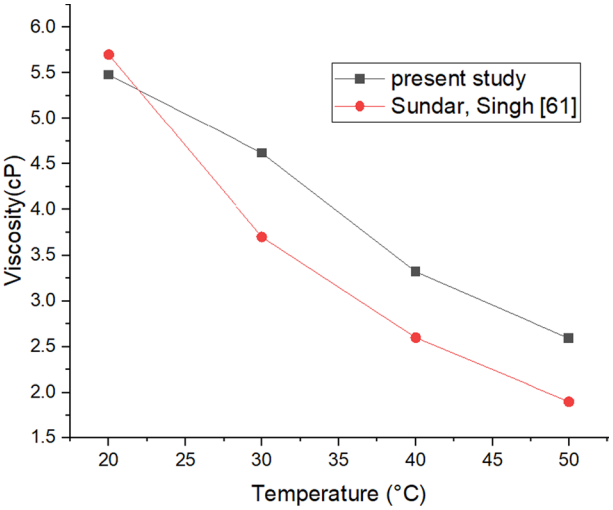

Fig. 7 Viscosity comparison of prepared base fluid at different temperatures

comparison of the study. The viscosity of the 60:40 (EG: W) fluid is nearly identical throughout a wide range of temperatures.

3.4 Density

Nanofluids' density equals the volume concentration of nanoparticles and the distilled water with ethylene glycol base fluid. The base fluid has an impact on density of nanofluids. The density of nanofluids is also affected by temperature. The density of nanofluid drops as the temperature rises. Figure 8 shows the density of nanofluids determined at 20 °C for the base fluid and varying volumetric concentrations of GNP and GNPs/CNC nanofluids. The density of base fluid result is in good accord with ASHRAE data, with a variance of less than 1 %.

According to the molecular dynamic simulation principle, the nanoparticles are filled with the molecules of the base fluid in various ways. In the case of nanofluids, increased van der Waals interaction causes nonuniform density to change in the interfacial region, resulting in the disparity in reported data. The density value is decreased for hybrid nanofluids (GNPs/CNC) when compared with single nanofluids (GNP). The density value of graphene nanoplatelets at 0.2 % volume fraction is 1304.2 $kg{\cdot}m^{-3}$ and at the same volume fraction for hybrid nanofluid of graphene nanoplatelets/cellulose nanocrystals (GNPs/CNC) is 1182.32 $kg{\cdot}m^{-3}$, respectively. It clearly shows density value increases with volume concentration. The density of the base fluid (water/ethylene glycol) compared with the 0.2 % concentration of graphene nanoplatelets is 18.6 %, and at the same concentration and temperature of hybrid nanofluid, it is 10.23 %. This confirms that density decreased for hybrid nanofluid when compared with single nanofluid composition. The nanofluid with a 0.02 % volume concentration and 70:30 Cu-GNP hybrid nanoparticles had the maximum density in research conducted by Kishore, Sireesha [81]. The author uses

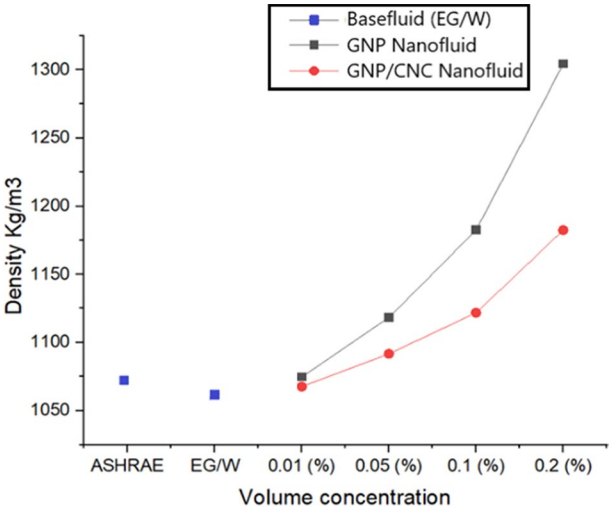

Fig. 8 Density of nanofluids at different concentrations (graphene nanoplatelets and hybrid GNPs/CNC)

a similar equation as in this study to compute the density of hybrid nanoparticles. Because copper has a higher density than graphene, the density (of 70:30 Cu-GNP) is higher concerning the author. A hybrid nanofluid's density is influenced by both the volume percentage and the densities of the nanoparticles. Following a similar trend in this research study, the density of the graphene nanoplatelets in single nanoparticle fluid is higher compared to hybrid nanofluid, as shown in the below figures of experimental density.

3.5 Specific Heat

Differential scanning calorimetry was used to investigate prepared nanofluids' specific heat capacity characteristics. Figure 9 shows the specific capacity of the base fluid, GNP and GNPs/CNC nanofluids. The hybrid nanofluids' effect of temperature and mass fraction on specific heat capacity for GNPs/CNC mass ratio is 1:1. There has not been enough mathematical and investigational research to estimate the nanofluid's specific heat capacity at various temperatures and volume concentrations. The specific heat capacity value of nanofluid samples is lower than that of base fluid, as shown in Fig. 9. The specific heat capacity of particles decreases as their volume concentration increases. At 30 °C, nanofluids' measured specific heat capacities are roughly 0.56 % and 7.52 % less than the base fluid for 0.01 and 0.2 volume per cent of nanoparticles, respectively. Most previous studies have shown that adding nanoparticles reduces the specific heat capacity, although some unexpected outcomes have also been recorded [82]. The heat capacity of nanofluids appears to be affected by the specific heat capacity of both nanoparticles and the base fluid. The interfacial energy released by solid–liquid is altered when suspended nanoparticles are adjusted. The surface free energy of nanoparticles influences the specific heat of nanocomposite materials since they have a higher surface area and a greater overall

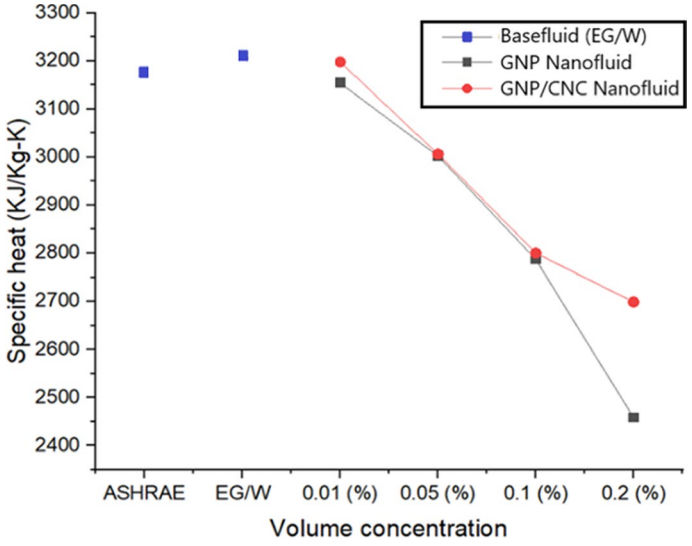

Fig. 9 GNP and GNPs/CNC specific heat capacity of nanofluids at different concentrations

heat capacity. On the one hand, this is due to the fact that water has a higher specific heat than nanoparticles; on the other hand, it demonstrates that the hybrid nanoparticle has a significant impact on specific heat capacity; even a small amount of mass fraction nanoparticle can significantly reduce specific heat capacity, especially at lower temperatures. The specific heats of the hybrid and single nanoparticle nanofluids, GNP (EG/W base fluid) nanofluid and GNPs/CNC (EG/W base fluid) hybrid nanofluid at 0.1 % are contrasted. It means that as the temperature rises, all specific heat capacities also rise. Besides water, it can be shown that hybrid nanofluid has the highest specific heat. This is due to the GNP's low specific heat capacity and the nanofluid's reduced GNPs/CNC concentration.

Specific heat capacity of 0.01 % and 0.2 % for single nanofluid (GNP) reduces by 1.74 % and 23.43 % compared to the base liquid. The specific heat of the hybrid nanofluid (GNPs/CNC) reduces by 0.38 % compared to 0.01 %, reducing by about 15.92 % at 0.2 %. The specific heat value when compared between hybrid nanofluid (GNPs/CNC) and single nanofluid (GNP) at 0.01 % is increased by 1.35 %, and at 0.2 %, it is increased by about 8.92 %. It can be concluded that the specific heat value is much higher for hybrid nanofluid than single nanofluid at lower volume concentration. The specific heat capacity of hybrid nanofluids has been demonstrated to be significantly affected by temperature. All studies universally agreed upon the reduced specific heat capacity of hybrid nanofluids compared to water [83]. According to a study, the temperature has a mixed effect on particular heat that is inconsistent. Fazeli, Emami [84] found that as the temperature of the multi-wall carbon nanotubes-copper oxide (MWCNT-CuO) increased from 20 °C to 35 °C, the specific heat capacity of the MWCNT-CuO reduced. A similar finding was made by Mousavi, Esmaeilzadeh [85], who found that the CuO/MgO/TiO_2 triple hybrid nanofluid had a decreasing SHC as temperature increased across all volume concentrations studied.

Few authors explained the effect of volume concentration on the specific heat capacity of hybrid nanofluids, exhibiting a linear relationship with the volume concentration of hybrid nanofluids. The combined influence of the specific heat capacities of the nanoparticles and base fluids is responsible for this tendency.

Furthermore, raising the volume concentration of nanoparticles appears to disrupt the solid–liquid phase's interfacial free energy. Because nanoparticles have a bigger surface area, their surface free energy has a stronger impact on overall heat power, influencing nanocomposite materials' specific heat [18, 82, 83]. When volume concentration was improved from 0.02 % to 0.06 % at the constant temperature of 20 °C, specific heat capacity decreased, showing a 7 % drop [44]. A similar trend was recorded in different studies [86, 87]. Their research also found that when the hybrid nanofluid's volume concentration increased, the hybrid nanofluid's specific heat capacity decreased significantly. As liquids (base fluids) have a greater specific heat capacity than solids (nanoparticles), the base fluids have more hybrid nanocomposites added to them that affect the specific heat capacity to drop, according to this analysis. When the volume concentration of the generated graphene-Al_2O_3 hybrid nanofluid was increased from 0.05 wt% to 0.15 wt% (relative to the base fluid at 20 °C), Gao, Xi [88] reported a specific heat capacity reduction of 4 to 7 %. At 30 °C, Fig. 10 depicts the fluctuation of specific heat capacity concerning the volume fraction of GNP loadings. The particular heat of nanofluid is shown to decrease as GNP loadings increase. Because GNP has a lower specific heat capacity than the base fluid, the specific heat capacity of the nanofluid decreased when GNP is added. The most significant reduction in specific heat is determined to be 8 % at 0.45 vol% by Selvam, Mohan Lal [70]. The specific heat capacity of the proposed nanofluid has a variation of 15 % decrement at 0.2 vol% with base fluid and reduces by 0.38 % as compared to 0.01 vol%. The thermal equilibrium-based rule of the mixture has developed after

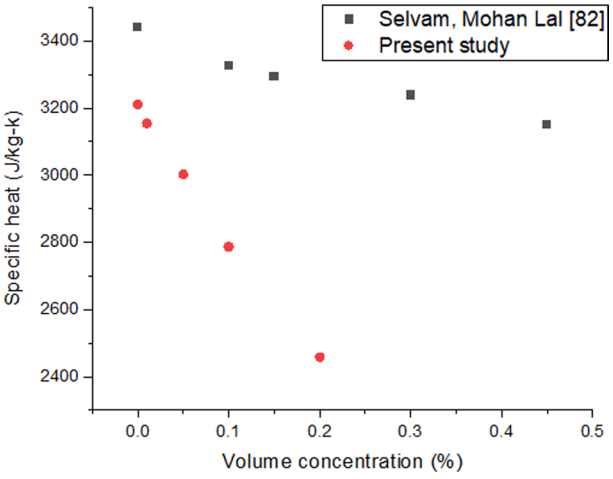

Fig. 10 Graphene nanoplatelet nanofluid comparison of specific heat at different concentrations with the literature

crossing 0.15 vol% of graphene nanoparticle addition, according to the author, and same observation is found in the present study due to the thermal diffusivity enhancement leading to the quick transmission of temperature. The decreasing trend of specific heat values similar to the present study is plotted in the image to validate the present study.

4 Conclusion

A two-step technique is used to prepare single and hybrid nanofluid of graphene nanoplatelet (GNP) and GNPs/CNC nanoparticles. Later the characteristic properties and thermophysical properties were studied at various volume concentrations in the base fluid of EG/water (60:40), with volume concentrations of 0.01 %, 0.05 %, 0.1 % and 0.2 %, and it was concluded that,

- All GNPs/CNC hybrid nanofluid samples give a thermal conductivity rise. At 0.2 vol% at 40 °C, investigational data reveal that thermal conductivity is enhanced by 27 %. At room temperature for GNP nanofluid, thermal conductivity values are in the range of 0.441 $W{\cdot}m^{-1}{\cdot}K^{-1}$, and for hybrid nanofluid, these are in the range of 0.515 $W{\cdot}m^{-1}{\cdot}K^{-1}$. The increase in the temperature decreased the viscosity of GNPs/CNC hybrid nanofluids. At 0.2 vol% of GNP nanofluid, the viscosity increased by 21 %. Similarly, there is an increase in viscosity by 24.5 % at 0.2 vol% of hybrid nanofluid (GNPs/CNC) at 20 °C compared to the base fluid.
- The experimental density of the nanofluid obtained was consistent with theoretical values. The density value of GNP and GNPs/CNC at 0.2 % volume concentration is 1304.2 $kg{\cdot}m^{-3}$ and 1182.32 $kg{\cdot}m^{-3}$, respectively, with an increase of 18.6 % and 10.23 % in comparison with the base fluid. The nanofluid's specific heat capacity drops with an increased nanoparticle volume fraction. At lower temperatures, the volume percentage of nanoparticles significantly impacts the particular heat of the hybrid nanofluid. The specific heat decreased with an increase in nanoparticle concentration. When compared with hybrid nanofluid (GNPs/CNC) and single nanofluid, there is an increase of 1.35 % and 8.92 % at 0.01 and 0.2 volume percentages, respectively.

The thermophysical characteristics of GNP and GNPs/CNC nanofluids obtained as a result suggest that this is a practical and useful approach for thermal engineering applications. Due to synergetic effects, GNPs/CNC hybrid-based nanoparticles revealed properties that could not be achieved independently using GNP or CNC nanoparticles. It is demonstrated that combining the diversity and uniqueness of both GNP and CNC enhances the number of applications available and provides undeniable benefits to their respective distinct characteristics. These hybrids have several features that make them suitable for sensing, electronics, optical, biomedical, energy storage and heat transfer applications.

Author Contributions MS was involved in conceptualization, visualization, investigation, data curation, writing—original draft preparation, reviewing and editing. DR was responsible for supervision, writing, reviewing and editing. KK, WSWH and RS contributed to writing, reviewing and editing.

Funding The authors appreciatively recognize University Malaysia Pahang (UMP) for the support financially and resources provided by Grant RDU 190194, FRGS/1/2018/TK03/UMP/02/26 and UMP Flagship RDU192204. The authors would also like to be grateful for the resources supplied by Sunway University.

Data Availability The corresponding author will provide the datasets produced and analysed during the current work upon reasonable request.

Declarations

Competing Interests The authors claim they are conscious and say no financial or personal conflicts that might have affected the research provided in this study.

References

1. J.J. Klemeš et al., Heat transfer enhancement, intensification and optimisation in heat exchanger network retrofit and operation. Renew. Sustain. Energy Rev. **120**, 109644 (2020)
2. H. Mohammed et al., Heat transfer and fluid flow characteristics in microchannels heat exchanger using nanofluids: a review. Renew. Sustain. Energy Rev. **15**, 1502–1512 (2011)
3. R. Saidur, K. Leong, H.A. Mohammed, A review on applications and challenges of nanofluids. Renew. Sustain. Energy Rev. **15**, 1646–1668 (2011)
4. D.D. Kumar, A.V. Arasu, A comprehensive review of preparation, characterization, properties and stability of hybrid nanofluids. Renew. Sustain. Energy Rev. **81**, 1669–1689 (2018)
5. M.A. Nazari et al., How to improve the thermal performance of pulsating heat pipes: a review on working fluid. Renew. Sustain. Energy Rev. **91**, 630–638 (2018)
6. S.U. Choi, J.A. Eastman, *Enhancing Thermal Conductivity of Fluids with Nanoparticles* (Argonne National Lab, Argonne, 1995)
7. M. Kibria et al., A review on thermophysical properties of nanoparticle dispersed phase change materials. Energy Convers. Manage. **95**, 69–89 (2015)
8. M. Jama et al., Critical review on nanofluids: preparation, characterization, and applications. J. Nanomater. **2016**, 1–22 (2016)
9. M. Sandhya et al., A systematic review on graphene-based nanofluids application in renewable energy systems: preparation, characterization, and thermophysical properties. Sustain. Energy Technol. Assess. **44**, 101058 (2021)
10. A. Leszczyńska et al., Polymer/montmorillonite nanocomposites with improved thermal properties: part I. Factors influencing thermal stability and mechanisms of thermal stability improvement. Thermochim. Acta **453**, 75–96 (2007)
11. M. Ibrahim et al., Comprehensive study concerned graphene nano-sheets dispersed in ethylene glycol: experimental study and theoretical prediction of thermal conductivity. Powder Technol. **386**, 51–59 (2021)
12. M.N.F.A. Malek, N.M. Hussin, N.H. Embong, P. Bhuyar, M.H.A. Rahim., N. Govindan, G.P Maniam. Ultrasonication: a process intensification tool for methyl ester synthesis: a mini review. Biomass Convers. Biorefin. 1–11 (2020)
13. P. Ares, K.S. Novoselov, Recent advances in graphene and other 2D materials. Nano Mater. Sci. **4**, 3–9 (2021)
14. I. Papanikolaou et al., investigation of the dispersion of multi-layer graphene nanoplatelets in cement composites using different superplasticiser treatments. Constr. Build. Mater. **293**, 123543 (2021)

15. M. Sandhya et al., ultrasonication an intensifying tool for preparation of stable nanofluids and study the time influence on distinct properties of graphene nanofluids—a systematic overview. Ultrason. Sonochem. **73**, 105479 (2021)
16. L.S. Sundar, M.K. Singh, A.C. Sousa, Enhanced heat transfer and friction factor of MWCNT–Fe3O4/water hybrid nanofluids. Int. Commun. Heat Mass Transf. **52**, 73–83 (2014)
17. T.R. Theres Baby, Sundara, Synthesis of silver nanoparticle decorated multiwalled carbon nanotubes-graphene mixture and its heat transfer studies in nanofluid. AIP Adv. **3**, 012111 (2013)
18. A. Amiri et al., Highly dispersed multiwalled carbon nanotubes decorated with Ag nanoparticles in water and experimental investigation of the thermophysical properties. J. Phys. Chem. C **116**, 3369–3375 (2012)
19. E. Watt et al., Hybrid biocomposites from polypropylene, sustainable biocarbon and graphene nanoplatelets. Sci. Rep. **10**, 1–13 (2020)
20. T. Li et al., Developing fibrillated cellulose as a sustainable technological material. Nature **590**, 47–56 (2021)
21. C.J. Chirayil, L. Mathew, S. Thomas, Review of recent research in nano cellulose preparation from different lignocellulosic fibers. Rev. Adv. Mater. Sci. **37** (2014)
22. M. Sandhya et al., Enhancement of the heat transfer in radiator with louvered fin by using graphene-based hybrid nanofluids. In: IOP Conference Series: Materials Science and Engineering. IOP Publishing (2021)
23. M. Sandhya et al., Enhancement of tribological behaviour and thermophysical properties of engine oil lubricant by graphene/Co-Cr nanoparticle additives for preparation of stable nanolubricant. In: IOP Conference Series: Materials Science and Engineering. IOP Publishing (2021)
24. Z. Hu et al., Stable aqueous foams from cellulose nanocrystals and methyl cellulose. Biomacromol **17**, 4095–4099 (2016)
25. D. Trache, V.K. Thakur, R. Boukherroub, Cellulose nanocrystals/graphene hybrids—a promising new class of materials for advanced applications. Nanomaterials **10**, 1523 (2020)
26. J.L. Sanchez-Salvador et al., Enhanced morphological characterization of cellulose nano/microfibers through image skeleton analysis. Nanomaterials **11**, 2077 (2021)
27. A. Dufresne, Nanocellulose: a new ageless bionanomaterial. Mater. Today **16**, 220–227 (2013)
28. P. Gupta et al., Low density and high strength nanofibrillated cellulose aerogel for thermal insulation application. Mater. Des. **158**, 224–236 (2018)
29. X. Chen et al., MXene/polymer nanocomposites: preparation, properties, and applications. Polym. Rev. **61**, 80–115 (2021)
30. G. Kadirgama et al., Graphene nanoplatelets–cellulose nanocrystals in engine oil for automotive applications. Green Mater. **40**, 1–9 (2022)
31. A.S.F. Mahamude et al., Experimental study on the efficiency improvement of flat plate solar collectors using hybrid nanofluids graphene/waste cotton. Energies **15**, 2309 (2022)
32. A.S.F. Mahamude et al., Numerical studies of graphene hybrid nanofluids in flat plate solar collector. In: 2021 International Congress of Advanced Technology and Engineering (ICOTEN). IEEE (2021)
33. P.K. Namburu et al., Viscosity of copper oxide nanoparticles dispersed in ethylene glycol and water mixture. Exp. Therm. Fluid Sci. **32**, 397–402 (2007)
34. M.M. Sarafraz et al., Thermal assessment of nano-particulate graphene-water/ethylene glycol (WEG 60: 40) nano-suspension in a compact heat exchanger. Energies **12**, 1929 (2019)
35. L.S. Sundar et al., Experimental investigation of thermo-physical properties, heat transfer, pumping power, entropy generation, and exergy efficiency of nanodiamond+ Fe3O4/60: 40% water-ethylene glycol hybrid nanofluid flow in a tube. Therm. Sci. Eng. Progress **21**, 100799 (2021)
36. R.P. Shankara et al., An insight into the performance of radiator system using ethylene glycol-water based graphene oxide nanofluids. Alex. Eng. J. **61**, 5155–5167 (2022)
37. A.I. Ramadhan, W.H. Azmi, R. Mamat, Stability and thermal conductivity of tri-hybrid nanofluids for high concentration in water-ethylene glycol (60: 40). Nanosci. Nanotechnol. Asia **11**, 121–131 (2021)
38. Z. Said et al., Thermophysical properties of water, water and ethylene glycol mixture-based nanodiamond+ Fe3O4 hybrid nanofluids: an experimental assessment and application of data-driven approaches. J. Mol. Liq. **347**, 117944 (2022)
39. K. Farhana et al., Experimental studies on thermo-physical properties of nanocellulose-aqueous ethylene glycol nanofluids. J. Adv. Res. Mater. Sci. **69**, 1–15 (2020)

40. T.-P. Teng, Y.-H. Hung, Estimation and experimental study of the density and specific heat for alumina nanofluid. J. Exp. Nanosci. **9**, 707–718 (2014)
41. A.I. Ramadhan, W.H. Azmi, R. Mamat, Experimental investigation of thermo-physical properties of tri-hybrid nanoparticles in water-ethylene glycol mixture. Walailak J. Sci. Technol. **18**, 9335 (2021)
42. M. Sandhya et al., Experimental study on properties of hybrid stable & surfactant-free nanofluids GNPs/CNCs (graphene nanoplatelets/cellulose nanocrystal) in water/ethylene glycol mixture for heat transfer application. J. Mol. Liq. **348**, 118019 (2022)
43. G. Kadirgama, A. Kumar, M. Sandhya, L. Samylingam, D. Ramasamy, K. Kadirgama,...& R. Saidur, (2022). Graphenenanoplatelets (GNPs)-cellulose nanocrystal (CNC) blended in SAE 40 hybrid engine oil for automotive applications. Green Materials.
44. H. Yarmand et al., Study of synthesis, stability and thermo-physical properties of graphene nanoplatelet/platinum hybrid nanofluid. Int. Commun. Heat Mass Transf. **77**, 15–21 (2016)
45. I. Kazemi, M. Sefid, M. Afrand, A novel comparative experimental study on rheological behavior of mono & hybrid nanofluids concerned graphene and silica nano-powders: characterization, stability and viscosity measurements. Powder Technol. **366**, 216–229 (2020)
46. W.S. Sarsam et al., Stability and thermophysical properties of non-covalently functionalized graphene nanoplatelets nanofluids. Energy Convers. Manage. **116**, 101–111 (2016)
47. A. Amiri et al., Backward-facing step heat transfer of the turbulent regime for functionalized graphene nanoplatelets based water–ethylene glycol nanofluids. Int. J. Heat Mass Transf. **97**, 538–546 (2016)
48. T.T. Baby, S. Ramaprabhu, Enhanced convective heat transfer using graphene dispersed nanofluids. Nanoscale Res. Lett. **6**, 289 (2011)
49. M. Kole, T. Dey, Investigation of thermal conductivity, viscosity, and electrical conductivity of graphene based nanofluids. J. Appl. Phys. **113**, 084307 (2013)
50. M. Mehrali et al., investigation of thermal conductivity and rheological properties of nanofluids containing graphene nanoplatelets. Nanoscale Res. Lett. **9**, 15 (2014)
51. H. Yarmand et al., Graphene nanoplatelets–silver hybrid nanofluids for enhanced heat transfer. Energy Convers. Manage. **100**, 419–428 (2015)
52. M.A. Marcos et al., PEG 400-based phase change materials nano-enhanced with functionalized graphene nanoplatelets. Nanomaterials **8**, 16 (2018)
53. J. Ganeshkumar et al., Experimental study on density, thermal conductivity, specific heat, and viscosity of water-ethylene glycol mixture dispersed with carbon nanotubes. Therm. Sci. **21**, 255–265 (2017)
54. S. Wu, O. Tahri, State-of-art carbon and graphene family nanomaterials for asphalt modification. Road Mater. Pavement Des. **22**, 735–756 (2021)
55. D.P. Kulkarni, D.K. Das, G.A. Chukwu, Temperature dependent rheological property of copper oxide nanoparticles suspension (nanofluid). J. Nanosci. Nanotechnol. **6**, 1150–1154 (2006)
56. J. Sobczak et al., Thermophysical profile of ethylene glycol based nanofluids containing two types of carbon black nanoparticles with different specific surface areas. J. Mol. Liq. **326**, 115255 (2021)
57. Z. Said et al., Stability, thermophysical and electrical properties of synthesized carbon nanofiber and reduced-graphene oxide-based nanofluids and their hybrid along with fuzzy modeling approach. Powder Technol. **364**, 795–809 (2020)
58. R. Vajjha, D. Das, B. Mahagaonkar, Density measurement of different nanofluids and their comparison with theory. Pet. Sci. Technol. **27**, 612–624 (2009)
59. M. O'neill, Measurement of specific heat functions by differential scanning calorimetry. Anal. Chem. **38**, 1331–1336 (1966)
60. K. Kodre et al., Differential scanning calorimetry: a review. Res. Rev.: J. Pharm. Anal. **3**, 11–22 (2014)
61. W. Su et al., Calibration of differential scanning calorimeter (DSC) for thermal properties analysis of phase change material. J. Therm. Anal. Calorim. **143**, 2995–3002 (2021)
62. T.J. Choi et al., Aqueous nanofluids containing paraffin-filled MWCNTs for improving effective specific heat and extinction coefficient. Energy **210**, 118523 (2020)
63. T. Batakliev et al., Effects of graphene nanoplatelets and multiwall carbon nanotubes on the structure and mechanical properties of poly (lactic acid) composites: a comparative study. Appl. Sci. **9**, 469 (2019)
64. M. Rashad et al., Effect of graphene nanoplatelets (GNPs) addition on strength and ductility of magnesium-titanium alloys. J. Magn. Alloys **1**, 242–248 (2013)

65. N. Usri et al., Thermal conductivity enhancement of Al2O3 nanofluid in ethylene glycol and water mixture. Energy Procedia **79**, 397–402 (2015)
66. S.K. Das et al., Temperature dependence of thermal conductivity enhancement for nanofluids. J. Heat Transf. **125**, 567–574 (2003)
67. A. Amiri et al., Laminar convective heat transfer of hexylamine-treated MWCNTs-based turbine oil nanofluid. Energy Convers. Manage. **105**, 355–367 (2015)
68. P. Keblinski et al., Mechanisms of heat flow in suspensions of nano-sized particles (nanofluids). Int. J. Heat Mass Transf. **45**, 855–863 (2002)
69. L.S. Sundar et al., Experimental investigation of the thermal transport properties of graphene oxide/Co3O4 hybrid nanofluids. Int. Commun. Heat Mass Transfer **84**, 1–10 (2017)
70. C. Selvam, D. Mohan Lal, S. Harish, Thermal conductivity and specific heat capacity of water–ethylene glycol mixture-based nanofluids with graphene nanoplatelets. J. Therm. Anal. Calorim. **129**, 947–955 (2017)
71. A. Ghozatloo, A. Rashidi, M. Shariaty-Niassar, Convective heat transfer enhancement of graphene nanofluids in shell and tube heat exchanger. Exp. Therm. Fluid Sci. **53**, 136–141 (2014)
72. N. Bing et al., 3D graphene nanofluids with high photothermal conversion and thermal transportation properties. Sustain. Energy Fuels **4**, 1208–1215 (2020)
73. S. Iranmanesh et al., evaluation of viscosity and thermal conductivity of graphene nanoplatelets nanofluids through a combined experimental–statistical approach using respond surface methodology method. Int. Commun. Heat Mass Transf. **79**, 74–80 (2016)
74. E.M.C. Contreras, G.A. Oliveira, E.P. Bandarra Filho, Experimental analysis of the thermohydraulic performance of graphene and silver nanofluids in automotive cooling systems. Int. J. Heat Mass Transf. **132**, 375–387 (2019)
75. Z. Wang et al., Experimental comparative evaluation of a graphene nanofluid coolant in miniature plate heat exchanger. Int. J. Therm. Sci. **130**, 148–156 (2018)
76. R. Bakhtiari et al., Preparation of stable TiO2-graphene/water hybrid nanofluids and development of a new correlation for thermal conductivity. Powder Technol. **385**, 466–477 (2021)
77. R. Taherialekouhi, S. Rasouli, A. Khosravi, An experimental study on stability and thermal conductivity of water-graphene oxide/aluminum oxide nanoparticles as a cooling hybrid nanofluid. Int. J. Heat Mass Transf. **145**, 118751 (2019)
78. G. Huminic et al., Study of the thermal conductivity of hybrid nanofluids: recent research and experimental study. Powder Technol. **367**, 347–357 (2020)
79. S. Rostami et al., Modeling the thermal conductivity ratio of an antifreeze-based hybrid nanofluid containing graphene oxide and copper oxide for using in thermal systems. J. Market. Res. **11**, 2294–2304 (2021)
80. C. Nguyen et al., Temperature and particle-size dependent viscosity data for water-based nanofluids–hysteresis phenomenon. Int. J. Heat Fluid Flow **28**, 1492–1506 (2007)
81. P. Kishore et al., Preparation, characterization and thermo-physical properties of Cu-graphene nanoplatelets hybrid nanofluids. Mater. Today: Proc. **27**, 610–614 (2020)
82. I. Shahrul et al., A comparative review on the specific heat of nanofluids for energy perspective. Renew. Sustain. Energy Rev. **38**, 88–98 (2014)
83. H. Adun et al., A critical review of specific heat capacity of hybrid nanofluids for thermal energy applications. J. Mol. Liq. **340**, 116890 (2021)
84. I. Fazeli, M.R.S. Emami, A. Rashidi, Investigation and optimization of the behavior of heat transfer and flow of MWCNT-CuO hybrid nanofluid in a brazed plate heat exchanger using response surface methodology. Int. Commun. Heat Mass Transf. **122**, 105175 (2021)
85. S. Mousavi, F. Esmaeilzadeh, X. Wang, Effects of temperature and particles volume concentration on the thermophysical properties and the rheological behavior of CuO/MgO/TiO2 aqueous ternary hybrid nanofluid. J. Therm. Anal. Calorim. **137**, 879–901 (2019)
86. A.A. Minea, Hybrid nanofluids based on Al2O3, TiO2 and SiO2: numerical evaluation of different approaches. Int. J. Heat Mass Transf. **104**, 852–860 (2017)
87. S. Akilu et al., Properties of glycerol and ethylene glycol mixture based SiO2-CuO/C hybrid nanofluid for enhanced solar energy transport. Sol. Energy Mater. Sol. Cells **179**, 118–128 (2018)
88. Y. Gao et al., Experimental investigation of specific heat of aqueous graphene oxide Al2O3 hybrid nanofluid. Therm. Sci. **25**, 515–525 (2021)

Authors and Affiliations

M. Sandhya[1,2] · D. Ramasamy[1,2,3,4] · K. Kadirgama[1,2,3,4] · W. S. W. Harun[1] · R. Saidur[5,6]

[1] Faculty of Mechanical and Automotive Engineering, Universiti Malaysia Pahang, 26600 Pekan, Pahang, Malaysia

[2] Advanced Nano Coolant Lubricant Laboratory (ANCoL),, Universiti Malaysia Pahang, 26600 Pekan, Pahang, Malaysia

[3] Centre of Excellence for Advanced Research in Fluid Flow (CARIFF), Universiti Malaysia Pahang, 26600 Pekan, Pahang, Malaysia

[4] Automotive Engineering Centre (AEC), Universiti Malaysia Pahang, 26600 Pekan, Malaysia

[5] Research Center for Nano-Materials and Energy Technology (RCNMET), School of Engineering and Technology, Sunway University, Bandar Sunway, 47500 Petaling Jaya, Selangor, Malaysia

[6] Department of Engineering, Lancaster University, Lancaster LA1 4YW, UK